Russian Geology and Geophysics © 2019, V.S. Sobolev IGM, Siberian Branch of the RAS
Vol. 60, No. 7, pp. 813–818, 2019 *DOI:10.15372/RGG2019061* *Geologiya i Geofizika*

Natural Thermal Convection in a Vertical Water-Filled Cylinder: Infrared Thermography Investigation

D.Yu. Demezhko✉, B.D. Khatskevich, M.G. Mindubaev

Institute of Geophysics, Ural Branch of the Russian Academy of Sciences, ul. Amundsena 100, Yekaterinburg, 620016, Russia

Received 14 March 2018; received in revised form 16 April 2018; accepted 25 April 2018

Abstract—Temperature logging furnishes the essential part of geothermal data. Its applications are progressively expanding due to advanced temperature loggers and data acquisition systems that ensure precise and stable measurements at high spatial and temporal resolution. However, it may be hard to achieve the full effect of the available logging facilities because of noisy temperature oscillations produced by natural convection in water-filled boreholes. A new laboratory method is suggested to study the structure of convection flows and their thermal effect by infrared thermography at conditions close to those of real temperature logging. Thermographic cameras image temperature anomalies on the outer wall of a water-filled pipe which are imprints of the convection processes in the water column. The temperature gradient on the pipe wall maintains flow of warm air ascending from a toroidal heater. It is shown experimentally using a pipe of 20 mm inner diameter that convection of fluid in the pipe forms a helical system rotating around a vertical axis at Rayleigh numbers in a range of 280 to 2800. As the Rayleigh numbers increase from 280 to 2800, the helical pitch decreases from 270 to 130 mm while the angular velocity increases from 0.7×10^{-2} to 3.4×10^{-2} rad/s. The experiment confirms the theoretically predicted dependence of standard deviation of temperature fluctuation on the temperature gradient and inner radius of the logged borehole: $\sigma_T = 3G \cdot r$.

Keywords: geothermics, convection, borehole, infrared thermography

INTRODUCTION

Temperature logging furnishes the greatest part of information for geothermal studies. Its applications are progressively expanding due to advanced temperature loggers and data acquisition systems that ensure precise and stable measurements at high spatial and temporal resolution. New applications appearing in addition to the conventional borehole thermometry address subtle effects in grounwater flow (Lapham, 1989; Anderson, 2005; Cermak et al., 2010; Pehme et al., 2014) or geodynamic processes in active seismic regions (Shimamura et al., 1985; Buntebarth et al., 2005; Demezhko et al., 2012a,b), which require high precision and temporal resolution of measurements. However, it may be hard to achieve the designed best performance of the logging facilities because of noisy temperature oscillations produced by natural thermal convection in water-filled boreholes. Therefore, the thermal effects of convection in boreholes are of both theoretical and practical interest.

Effects of fluid convection on borehole temperature patterns were discussed in many publications (Diment, 1967; Gretener, 1967; Sammel, 1968; Devyatkin and Kutasov, 1973; Urban et al., 1978; Solodov et al., 2002; Cermak, 2009; Cermak et al., 2008a; Demezhko et al., 2012a). Yet, experimental *in situ* convection studies are problematic: it is difficult to set up the appropriate experimental conditions (borehole diameter, temperature, temperature gradient, Rayleight number) and to avoid the influence of sensors and cables. In this respect, a laboratory experiment can be complementary to field borehole measurements.

Natural thermal convection in borehole water columns is commonly studied in laboratory using a thermally insulated glass pipe filled with water which is heated from below to maintain the temperature gradient (Ostroumov, 1958; Berthold and Börner, 2008; Berthold and Resagk, 2012). This setting differs from the field conditions where the temperature gradient results from heat exchange with the drilled rocks. The convection currents are monitored either by temperature sensors embedded into the pipe (Ostroumov, 1958) or by photo or video imaging of particles visible through the glass walls (Ostroumov, 1958; Berthold and Börner, 2008; Berthold and Resagk, 2012). In the former case, the resolution is limited by the number of sensors which, moreover, may interfere with the convection process. The latter technique is workable in estimating the velocity of flow but it fails to image its spatial structure. Some of the disadvantages are overcome in a new laboratory method we suggest for modeling borehole convection.

PROBLEM FORMULATION

Natural convection in boreholes is driven by the positive temperature gradient which causes stratification into warmer

✉Corresponding author.
E-mail adress: ddem54@inbox.ru (D.Yu. Demezhko)

(lighter) and colder (heavier) fluids. Ascending and descending flows tend to equalize the density and temperature heterogeneity, but the temperature field of rocks maintains the positive gradient.

The onset and behavior of convection depend on the dimensionless Rayleigh number. For borehole conditions (vertical cylinder):

$$Ra = \frac{g\beta r^4}{va} G, \quad (1)$$

where g is the acceleration due to gravity, β is the thermal expansion coefficient; ν is the kinematic viscosity; a is the thermal diffusivity; r is the borehole radius; G is the temperature gradient. The parameters β, ν, and a, in their turn, are temperature-dependent. The critical Rayleigh number Ra_{crit} required for the onset of convection is in the range 68 to 216 depending on the thermal conductivity ratio λ_f/λ_m between the fluid and the surrounding rock masses (Gershuni and Zhukhovitskii, 1976):

$$Ra_{crit} = \frac{96}{5(1+7\lambda_f/\lambda_m)}\left[3(33+103\lambda_f/\lambda_m) - \sqrt{3(2567+14794\lambda_f/\lambda_m+26927(\lambda_f/\lambda_m)^2)}\right]. \quad (2)$$

Ra_{crit} = 68 and ($\lambda_f/\lambda_m \to \infty$) if the borehole is thermally insulated (zero conduction) and Ra_{crit} = 216 (λ_f/λ_m = 0) if the rock mass is an ideal heat conductor.

The onset of convection can be also defined via the critical temperature gradient (Diment, 1967; Gretener, 1967):

$$G_{crit} = \frac{g\beta T}{C} + \frac{Bva}{g\beta r^4}, \quad (3)$$

where T is the absolute temperature, C is the specific heat, β is the thermal expansion coefficient, B is the constant corresponding to the critical Rayleigh number at large aspect ratios of boreholes (length-to-diameter ratio). The first term in (3) is the adiabatic gradient which is quite low (~10^{-4} K/m) for water-filled boreholes and the second one refers to fluid viscosity and hole radius.

METHODS

The structure of convection currents can be studied by infrared thermography of the outer wall of a water-filled ceramic pipe. Thermographic cameras image temperature anomalies which arise in the water column once the temperature gradient exceeds the critical value (equation 3) and are imprinted on the pipe wall. As it was found out experimentally, the interior temperature perturbations are best transferred to the walls of mullite-ceramic pipes. The measurements were performed using a specially designed laboratory system (Fig. 1).

The system consists of a water-filled ceramic cylinder (*1*) upright on a stand (*2*), with a temperature gradient on its outer wall maintained by an ascending air flow (*3*) from a toroidal heater (*4*); a movable thermographic camera (*5*) to image the space and time temperature patterns; and two thermocouples (*6*) mounted on the inner wall and connected to the recorder (*7*) to measure temperature. The camera (5) can be moved vertically, horizontally, and around the cylinder (within ± π/2).

The critical temperature gradient in real boreholes, 75 to 150 mm in diameter, is normally as low as (10^{-3}–10^{-5}) K/m and hardly can be maintained in laboratory against the 10^{-1}–10^{0} K/m natural background (negative temperature gradient in air). However, it is much higher in pipes of a smaller diameter. Specifically, it was ~1 K/m in the 1 m long pipe with an inner diameter of 20 mm we used in the experiments. The range of temperature oscillations associated with convection likewise increases proportionally to the gradient (Sammel, 1968; Diment and Urban, 1983; Eppelbaum and Kutasov, 2011; Demezhko et al., 2017), which allows stable thermal imaging even at a modest temperature resolution of ~0.1 K. On the other hand, the laboratory results for small

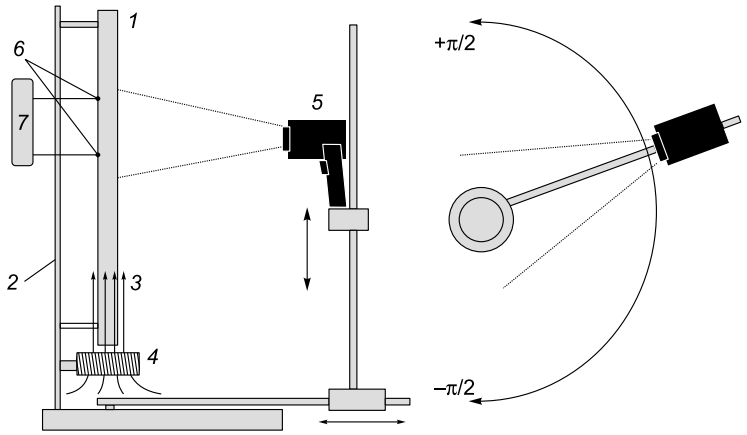

Fig. 1. Laboratory system for modeling natural convection in a water-filled borehole. Side (left) and top (right) view. See text for explanation.

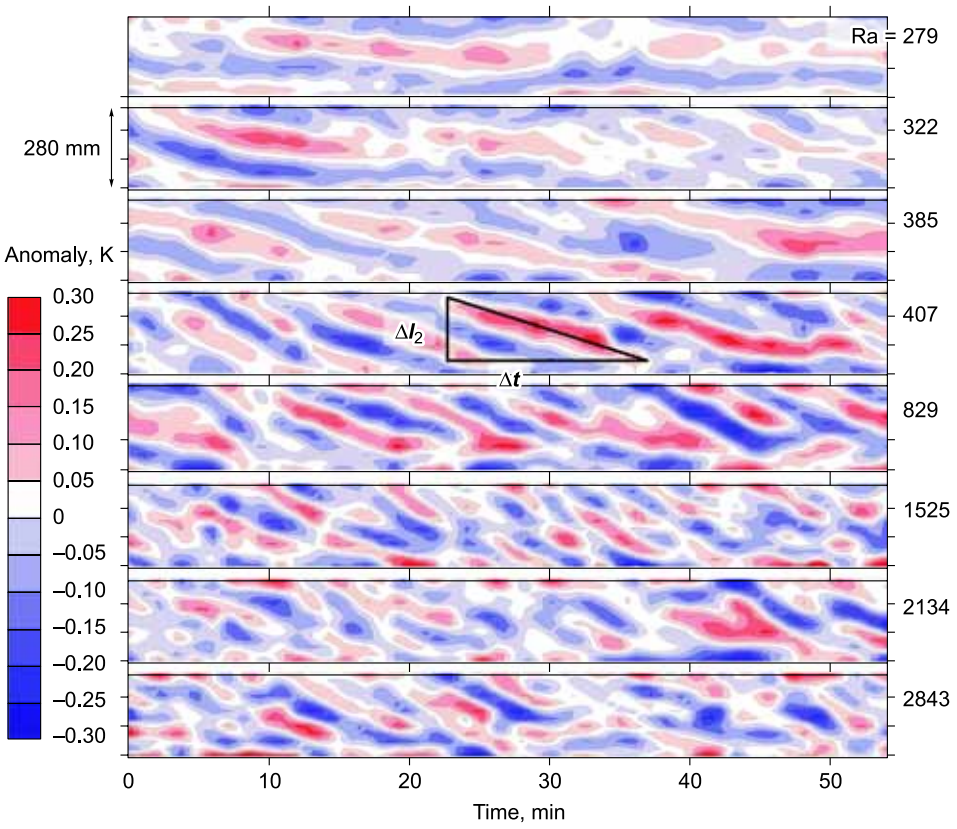

Fig. 2. Time-dependent temperature anomalies caused by thermal convection in a vertical water-filled pipe at different Rayleigh numbers, with an example of estimating the dip of anomalies η_2.

pipes can be extrapolated to the real borehole conditions by the similarity law.

Temperature anomalies were measured in the central part of the cylinder using a *Testo 875* thermal imager, after two-hour heating and onset of stable convection, at a specified camera position. The temperature gradient was controlled by varying the heater power. The measurements lasted 45 min, at a sampling rate of 1 min, and yielded images of temperature anomalies varying with time (Fig. 2) or with azimuth angle (Fig. 3). The anomalies on the cylinder wall were estimated for the central profile of each image by subtraction of the unperturbed temperature distribution corresponding to the average temperature gradient from the observed distribution. The azimuth-dependent temperature anomalies (from $-\pi/2$ to $+\pi/2$ at every $\pi/4$) were imaged before, during (16th and 31st min), and after the monitoring run (see Fig. 3 for the record at the 16th min of monitoring).

RESULTS AND INTERPRETATION

Stable temperature heterogeneity on the pipe outer wall shows up since Ra = 279. Inclined azimuth-dependent anomalies (Fig. 3) indicate that the ascending and descend-

Table 1. Infrared thermography: experimental conditions and average convection parameters

Experimental conditions			Average values of convection parameters					
N	Number of estimates	Heater power, *W*	Temperature, *T*, °C	Gradient, *G*, K/m	Rayleigh number, *Ra*	Helical pitch *h*, mm	Angular velocity ω, rad/s	Period τ, s
1	4	11.1	29.9	1.12	279	257	No rotation	
2	5	17.4	28.6	1.65	385	276	0.0071	882
3	2	25.0	24.1	1.76	322	214	0.0126	498
4	4	34.0	24.6	2.16	407	222	0.0162	386
5	5	44.4	25.4	4.19	829	193	0.0186	337
6	4	56.3	32.0	5.58	1525	127	0.0316	199
7	5	69.4	35.4	6.86	2134	157	0.0291	216
8	3	84.0	35.6	9.08	2843	152	0.0344	183

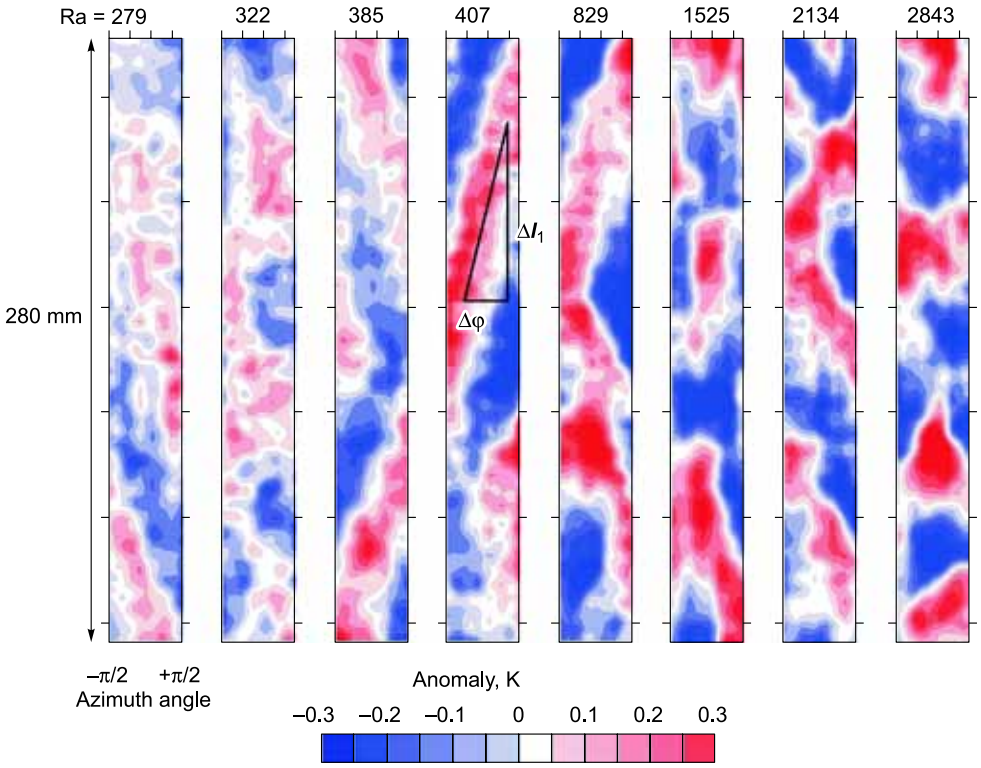

Fig. 3. Azimuth-dependent temperature anomalies caused by convection in a vertical water-filled pipe at different Rayleigh numbers, with an example of estimating the dip of anomalies η_1.

ing flows are organized as a system of helical jets. The time-dependent inclined anomalies (Fig. 2) are clearly manifested at $Ra \geq 322$ and indicate the rotation of the entire helical system around the cylinder axis. The parameters of the helical system can be quantified by estimating the dip of the anomalies. The dip of azimuth-dependent anomalies $\eta_1 = \Delta l_1/\Delta\varphi$ controls the direction of helical twist (right at $\eta_1 > 0$ and left at $\eta_1 < 0$) and pitch ($h = 2\pi\ \eta_1$). The dip ($\eta_2 = \Delta l_2/\Delta t$) and helical pitch ($h$) allow estimating the rotation period $\tau = h/\eta_2 = 2\pi\eta_1/\eta_2$ or angular velocity $\omega = 2\pi/\tau = \eta_2/\eta_1$ of the system. Two to five estimates of T, G, Ra, ω, τ, and h were obtained in each test, depending on the number of time- and azimuth-dependent anomaly pairs with clearly detectable axes (Table 1).

As shown by the experiments, the convection currents form a rotating helical system once the Rayleigh number exceeds at least slightly the critical value. This value (equation 2) is hard to constrain precisely for the given experimental system without knowing the thermal conductivity of rocks. However, thermal conductivity can be only taken as an effective value that accounts for convective heat exchange between the outer pipe wall and the air flow. The critical Rayleigh number is expected to approach the upper limit ($Ra_{crit} = 216$) in our case, because convective heat transfer is much more efficient than conduction.

The thermography data were used to obtain a 3D model of natural convection in boreholes (Fig. 4). The model represents systems of two or four helical currents similar to the asymmetric localization of convection flows by Gershuni and Zhukhovitskii (1976). However, although looking asymmetrically in the section view, the system actually has a higher-order helical symmetry.

The helical currents observed in the experiments were right or left helixes at equal probability, and had a pitch

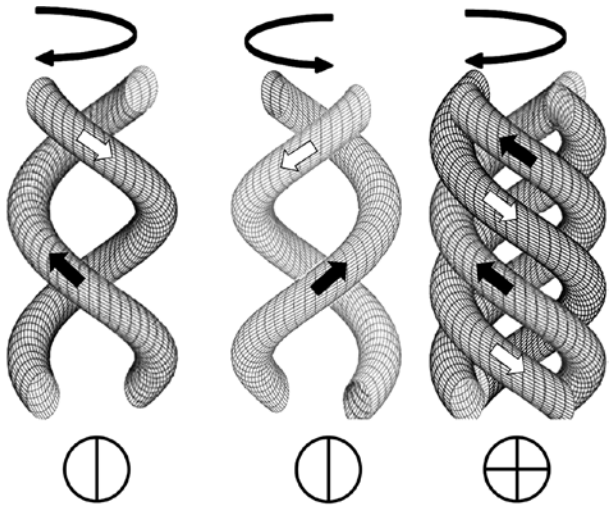

Fig. 4. 3D model of convection flows. Black and white arrows are ascending and descending flows. Arrows on top show the direction of helical twist. Circles below show possible version of asymmetric localization of convection flows in the hole cross section, after (Gershuni and Zhukhovitskii, 1976).

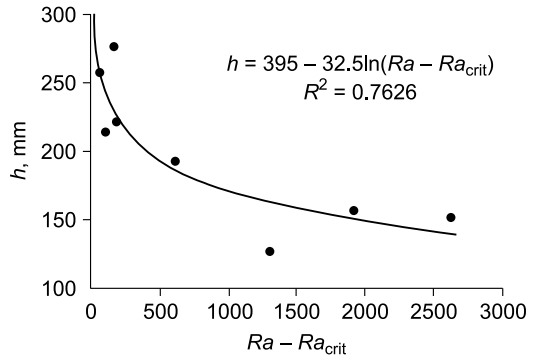

Fig. 5. Helical pitch h as a function of Rayleigh number supercriticality.

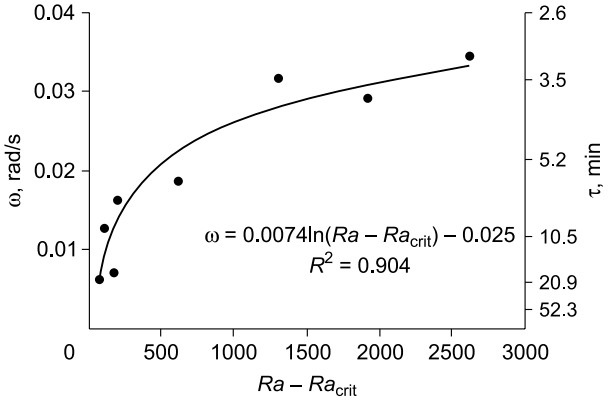

Fig. 6. Angular velocity (ω) and rotation period (τ) of the helical system as a function of Rayleigh number supercriticality.

from 127 to 276 mm. As the Rayleigh number increased progressively above the critical value, the helical pitch decreased, i.e., the helical became compressed (Fig. 5) while the angular velocity increased from zero at Ra = 294 to an average of 7×10^{-3} rad/s ($\tau \approx 15$ min) at Ra = 347 and finally to 34×10^{-3} rad/s at Ra = 2843 ($\tau \approx 3$ min). The dependence of the angular velocity on the supercriticality of the Rayleigh number is well approximated by a logarithmic curve (Fig. 6). The rate of angular velocity increase reduces progressively, possibly, as a result of viscous friction. The direction of rotation was found out to agree with the direction of helical twist: it was counterclockwise for the right helicons and clockwise for the left ones (view from above).

Temperature variations inside the cylinder (on the inner wall) were measured by thermocouples. The standard deviation of temperature variations in the Ra = 500–20,000 range was found out to depend on the temperature gradient G and the cylinder inner radius r (Fig. 7). This result agrees with the previous prediction by modeling for natural convection in a channel of square section: $\sigma_T = 3G \cdot r$, where r is the channel half-width (Demezhko et al., 2017).

DISCUSSION AND CONCLUSIONS

A novel laboratory method is suggested to study the structure of natural convection currents in water-filled boreholes in conditions similar to the real field setting. It implies thermal imaging of temperature anomalies on the outer wall of a ceramic cylinder filled with water and heated from below, with ascending air flow from the heater maintaining temperature gradient and convection.

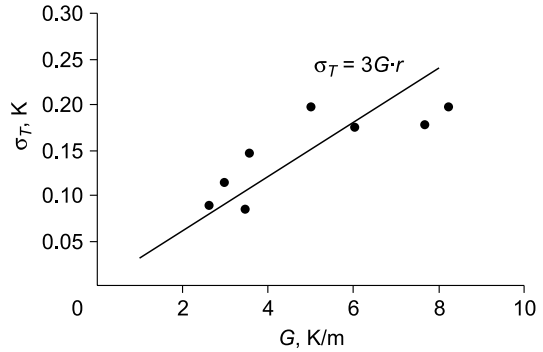

Fig. 7. Standard deviation of temperature fluctuations as a function of temperature gradient (for a pipe with an inner radius of r = 10 mm). Straight line is theoretical dependence according to (Demezhko et al., 2017).

According to the existing views (Diment and Urban, 1983; Berthold and Börner, 2008; Cermak et al., 2008b), convection currents form vertical series of convective cells (like the Rayleigh–Bénard cells in a plane layer). However, natural convection in pipes can appear as helical systems, as it was predicted earlier by modeling (Khoroshev, 2012; Mindubaev and Demezhko, 2012; Demezhko et al., 2017) and proven experimentally in this study for the first time. The helical convection currents rotate around a vertical axis, with their angular velocity increasing and helical pitch decreasing as the Rayleigh number increases. It means that the concepts of convective cell and its vertical size used to describe the temperature effects of convection are inappropriate for the convection structure in boreholes. The ratio of the convective cell height to the borehole radius (dimensionless constant A) was used in the equation $\Delta T_{max} = A \cdot G \cdot r$ suggested to estimate the maximum range of temperature oscillations (Diment and Urban, 1983). However, no reliable estimates of the cell height have been obtained since then.

The wrong idea of the convection structure has been used in all known tools for reducing convection in boreholes. In these methods, temperature measurements in boreholes are isolated with packers (Beck et al., 1971; Colombani et al., 2016) or horizontal discs (Harries and Ritchie, 1981; Vroblesky et al., 2006) which divide the borehole into intervals smaller than the vertical size of convection cells. Meanwhile, our experimental study shows that convection currents are not limited vertically by the cell size. In this respect, convection in boreholes can be better suppressed by using vertical rather than horizontal dividers, which can reduce the effective hole radius and the Rayleigh number and thus prevent rotation of the helical convection system.

REFERENCES

Anderson, M.P., 2005. Heat as a ground water tracer. Ground Water 43 (6), 951–968.

Beck, A.E., Anglin, F.M., Sass, J.H., 1971. Analysis of heat flow data—in situ thermal conductivity measurements. Can. J. Earth Sci. 8, 1–19.

Berthold, S., Börner, F., 2008. Detection of free vertical convection and double-diffusion in groundwater monitoring wells with geophysical borehole measurements. Environ. Geol. 54 (7), 1547–1566.

Berthold, S., Resagk, C., 2005. Investigation of thermal convection in water columns using particle image velocimetry. Experiments in Fluids 52 (6), 1465–1474.

Buntebarth, G., Chelidze, T., Middleton, M., 2005. Time-Dependent Microtemperature and Hydraulic Signals Associated with Tectonic/Seismic Activity. Tbilisi, pp. 4–108.

Cermak, V., 2009. Recurrence quantification analysis of borehole temperatures: evidence of fluid convection. Int. J. Bifurcation and Chaos 19 (3), 889–902.

Cermak, V., Safanda, J., Bodri, L., 2008a. Precise temperature monitoring in boreholes: Evidence for oscillatory convection? Part I. Experiments and field data. Int. J. Earth Sci. 97 (2), 365–373, doi:10-1007/s00531-007-0237-4.

Cermak, V., Bodri, L., Safanda, J., 2008b. Precise temperature monitoring in boreholes: evidence for oscillatory convection? Part II: theory and interpretation. Int. J. Earth Sci. 97 (2), 375–384.

Cermak, V., Safanda, J., Bodri L., 2010. Thermal instability of the fluid column in a borehole: application to the Yaxcopoil hole (Mexico). Int. J. Earth Sci. 99 (6), 1437–1451.

Colombani, N., Giambastiani, B.M.S., Mastrocicco, M., 2016. Use of shallow groundwater temperature profiles to infer climate and land use change: interpretation and measurement challenges. Hydrological Processes 30 (14), 2512–2524.

Devyatkin, V.N., Kutasov, I.M., 1973. Effect of free thermal convection and casing on borehole temperature field, in: Heat Fluxes from Crust and Upper Mantle [in Russian], Nauka, Moscow, pp. 99–106.

Demezhko, D.Yu., Yurkov, A.K., Utkin, V.I., Klimshin, A.V., 2012a. On the nature of temperature variations in borehole kun-1 (Kunashir Island). Russian Geology and Geophysics (Geologiya i Geofizika) 53 (3), 313–321 (406–414).

Demezhko, D.Yu., Yurkov, A.K., Utkin, V.I., Shchapov, V.A., 2012b. Temperature changes in the KUN-1 borehole, Kunashir Island, induced by the Tohoku earthquake (March 11, 2011, M = 9.0). Dokl. Earth Sci. 445, 1 (2), 883–887.

Demezhko, D.Yu., Mindubaev, M.G., Khatskevich, B.D., 2017. Thermal effects of natural convection in boreholes. Russian Geology and Geophysics (Geologiya i Geofizika) 58 (10), 1270–1276 (1602–1610).

Diment, W.H., 1967. Thermal regime of a large diameter borehole: instability of the water column and comparison of air- and water-filled conditions. Geophysics 32, 720–726.

Diment, W.H., Urban, Th.C., 1983. A simple method for detecting anomalous fluid motions in boreholes from continuous temperature logs. GRC Trans. 7, 485–490.

Eppelbaum, L.V., Kutasov, I.M., 2011. Estimation of the effect of thermal convection and casing on the temperature regime of boreholes: a review. J. Geophys. Eng. 8 (1), 1–10.

Gershuni, G.Z., Zhuhovitskii, E.M., 1976. Convective Stability of Incompressible Fluids. Keter Publishing House, Jerusalem.

Gretener, P.E., 1967. On the thermal instability of large diameter wells—an observational report. Geophysics 32, 727–738.

Harries, J.R., Ritchie, A.I.M., 1981. The use of temperature profiles to estimate the pyritic oxidation rate in a waste rock dump from an opencut mine. Water, Air and Soil Pollution 15 (4), 405–423.

Khoroshev, A.S., 2012. Natural convection currents in long vertical cylindrical zones at a constant vertical temperature gradient on the lateral surface. Bull. Samara State Aerospace University 36 (5–1), 46–48.

Lapham, W.W., 1989. Use of Temperature Profiles Beneath Streams to Determine Rates of Vertical Ground-Water Flow and Vertical Hydraulic Conductivity. US Geological Survey Water-Supply Paper 2337.

Mindubaev, M.G., Demezhko, D.Yu., 2012. Natural convection in boreholes: numerical modeling and experimental constraints. Monitoring. Nauka i Tekhnologii 13 (4), 12–18.

Ostroumov, G.A., 1958. Free Convection under the Conditions of the Internal Problem. NACA Technical Memorandum, No. 1407.

Pehme, P.E., Parker, B.L., Cherry, J.A., Blohm, D., 2014. Detailed measurement of the magnitude and orientation of thermal gradients in lined boreholes for characterizing groundwater flow in fractured rock. J. Hydrology 513, 101–114.

Sammel, E.A., 1968. Convective flow and its effect on temperature logging in small-diameter wells. Geophysics 33 (6), 1004–1012.

Shimamura, H., Ino, M., Hikawa, H., Iwasaki, T., 1985. Groundwater microtemperature in earthquake regions. Pure and Applied Geophysics 122 (6), 933–946.

Solodov, I., Malkovsky, V., Pek, A., Benson, S., 2002. New evidence for the combined influence of vapor condensation and thermal convection on groundwater monitoring wells. Environ. Geol. 42 (2–3), 145–150.

Vroblesky, D.A., Casey, C.C., Lowery, M.A., 2006. Influence of In-Well Convection on Well Sampling. Scientific Investigations Report 5247. Dept. of the Interior, U.S. Geological Survey.

Urban, T.C., Diment, W.H., Nathenson, M., 1978. East Mesa geothermal anomaly, Imperial County, California: Significance of temperatures in a deep drill hole near thermal equilibrium. Geothermal Resources Council Transactions 2 (2), 667–670.

Editorial responsibility: A.D. Duchkov